ACS OMEGA

Open Access

http://pubs.acs.org/journal/acsodf

Article

Soybean-Based Bio-Adhesives: Role of Diamine on the Adhesive Properties

Uday Panchal, Mayankkumar L. Chaudhary, Pratik Patel, Jainishkumar Patel, and Ram K. Gupta*

Cite This: *ACS Omega* 2024, 9, 10738−10747

Read Online

ACCESS | Metrics & More | Article Recommendations | Supporting Information

ABSTRACT: One possible approach to achieving sustainable development in the materials sector is to produce polymers from plant oils (POs), which are renewable and environmentally beneficial. Polymers with a high concentration of functional groups can be used as cross-linking agents to enhance the properties of epoxidized POs (epoxidation of plant oil)-based polymers. In this work, a unique resin with novel properties and potential uses was produced by cross-linking epoxidized soybean oil (ESO) with branched and flexible polyamines by ring-opening and amidation polymerizations. This approach is straightforward and ecologically benign. After curing, melamine pentane diamine (MPD) polymer maintained its position as the strongest structural adhesive among the synthesized resins, with a bonding strength of almost 2000 kPa for stainless steel; irrespective of the temperature, stainless steel consistently outperforms melamine ethylene diamine-ESO resin in strength comparisons. At 100 °C, stainless steel has a lap shear strength of about 300 kPa, which is far higher than copper and aluminum; at 180 °C, this value increases by another 750 kPa. While MPD-ESO resin has a shear strength of 1996 kPa at 180 °C, melamine butane diamine-ESO resin has a shear strength of only 1220 kPa.

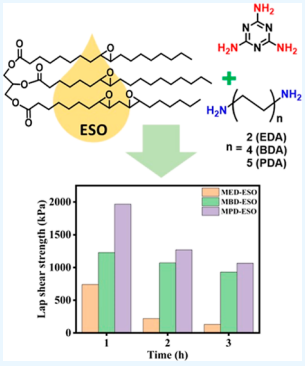

1. INTRODUCTION

The aerospace, automotive, marine, infrastructural, medical device, consumer goods, and sports equipment industries are just a few examples of how polymers have become indispensable modern materials. Polymers have many advantages over other materials, including the capacity to be modified in various ways, being simple to manufacture, having a high strength-to-weight ratio, being resistant to chemical and physical deterioration, and being inexpensive.[1−9] Triglyceride oils have some of the best properties because of their inexpensive price, relatively simple processing, and chemical functionality.[10] Triglyceride oils are the focus of a worldwide effort to create novel monomers and polymers with physical and thermo-mechanical qualities comparable to or even superior to those of their petrochemical counterparts.[11,12] Despite the presence of hydroxyls and epoxies in vegetable oils' fatty acid chains, which can be used directly for polymerization, the oils' functionalities are generally too low to find widespread usage.[13,14] Chemical alteration of the naturally occurring reactive sites that exist in triglycerides (such as ester groups and carbon−carbon double bonds) is necessary for the majority of vegetable oils before they can be used as desirable monomers for polymer synthesis.[10] Here, hydroformylation/hydrogenation, transesterification/amidation, acrylation, and epoxidation are a few of the methods available for modifying oils derived from plants. Two processes (epoxidation and ring opening) are required for the acrylation or methacrylation of vegetable oils for successful modification. Soybean oil has increased acrylic functionality (all the way up to five per triglyceride) due to its structural strain. Also, because of this, epoxides have reactive and flexible functional groups. Thus, epoxidation of plant oils (EPOs), can supply reactive monomers for sustainable polymer synthesis.[15] EPO cross-linking is the best way to improve polymerized materials. There are two approaches in the literature. Cross-linking POs directly or after premodifications are the two main ways to achieve the significant properties of polymeric material. In direct cross-linking, tiny molecules can cure or harden polymers. These molecules include carboxylic acids,[16,17] small amines,[18−20] and anhydrides.[21] Micro cross-linkers have short chains, low molecular weight, and restricted functionality; hence, their products have weak mechanical strength and thermal stability.

The characteristics of polymers based on EPO are improved by using large cross-linking agents (such as polymers) that are rich in functional groups. Some examples include polylactic acid,[22] tannin acid,[23] and doubly esterified starch.[24] Improved thermal and mechanical properties were observed after polymeric cross-linkers were added to the resulting thermosets, suggesting possible uses in structural materials.[25] To speed up the process of making polymeric materials, it is possible to make changes before cross-linking that will result in highly

Received: December 3, 2023
Revised: January 18, 2024
Accepted: February 12, 2024
Published: February 21, 2024

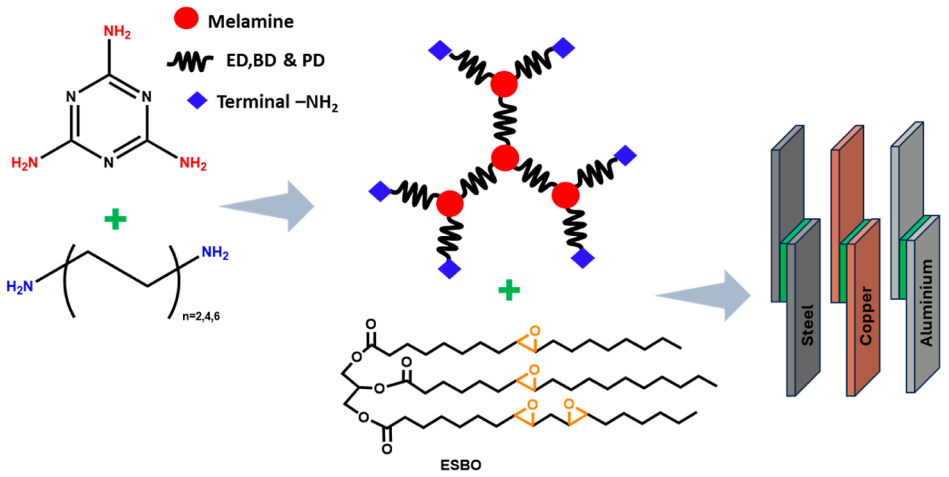

Figure 1. Schematic diagram for the synthesis of MED-ESO resin, MBD-ESO resin, and MPD-ESO resin.

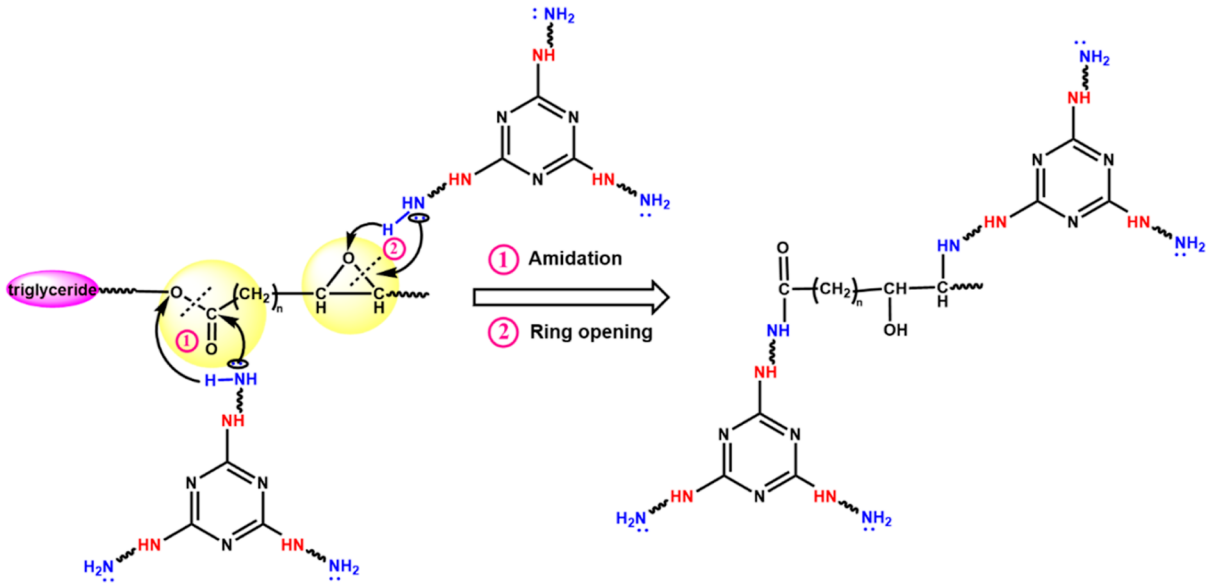

Figure 2. Reaction mechanism of the formation of resin using amine and ESO.

reactive intermediate products. There are many reports of EPOs being cross-linked after being converted to cyclic carbonates[24,26,27] or acrylate derivatives.[28] Direct cross-linking without changes is the superior option since it maximizes the usefulness of EPOs at the lowest possible cost. High-performance materials, however, are still hard to produce because of a lack of appropriate cross-linkers.

Epoxy groups[29] often situated in the internal positions of long carbon chains, present a challenge for curing EPOs due to steric hindrance, which slows down the interaction between the cross-linker and the epoxy groups. Thus, cross-linkers with many functional groups should potentially improve the statistical likelihood of cross-linking processes. In addition, the cross-linker's functional groups would be easier to reach if the chains were longer and more flexible. Finally, the triglyceride structure is a reactive site that supplies extra cross-linking sites besides the epoxy groups. To test this theory, we have synthesized three different flexible polymers, such as melamine ethylene diamine (MED) polymer, melamine butane diamine (MBD) polymer, and melamine pentane diamine (MPD) polymer, by using ethylene diamine (EDA), butane diamine (BDA), pentane diamine (PDA), and melamine (MA), as the cross-linkers for epoxidized soybean oil (ESO). The cross-linking degree as well as the mechanical properties of polyamines are higher compared to those of small amines.[18,19] These polymers' very flexible chains made reactive sites easily accessible, and the abundant aliphatic amino groups in them reacted with the epoxy group and triglyceride. The results of this research show that the MED-ESO, MBD-ESO, and MPD-ESO resins have remarkable properties and broad application potential, such as adhesives. Figure 1 shows the schematics of the reaction and its application as an adhesive.

2. MATERIALS AND METHODS

2.1. Materials. Soybean oil was purchased from a local Walmart (Pittsburgh, KS, USA). BDA (99%), EDA (99%), and PDA (99%) were purchased from Acros Organics, (NJ, USA) and used as received. MA (99%) was purchased from Alfa Aesar (Ward Hill, MA, USA). Ammonium chloride (99%) was purchased from Fisher Scientific (Fair Lawn, NJ, USA).

2.1.1. Synthesis of MED, MBD, and MPD Polymer. To prepare the MED polymer, EDA and MA were mixed under stirring at 50 °C. Then, 6% NH_4Cl (based on the weight of MA) was added, and the reaction mixture was heated to 195

https://doi.org/10.1021/acsomega.3c09650
ACS Omega 2024, 9, 10738−10747

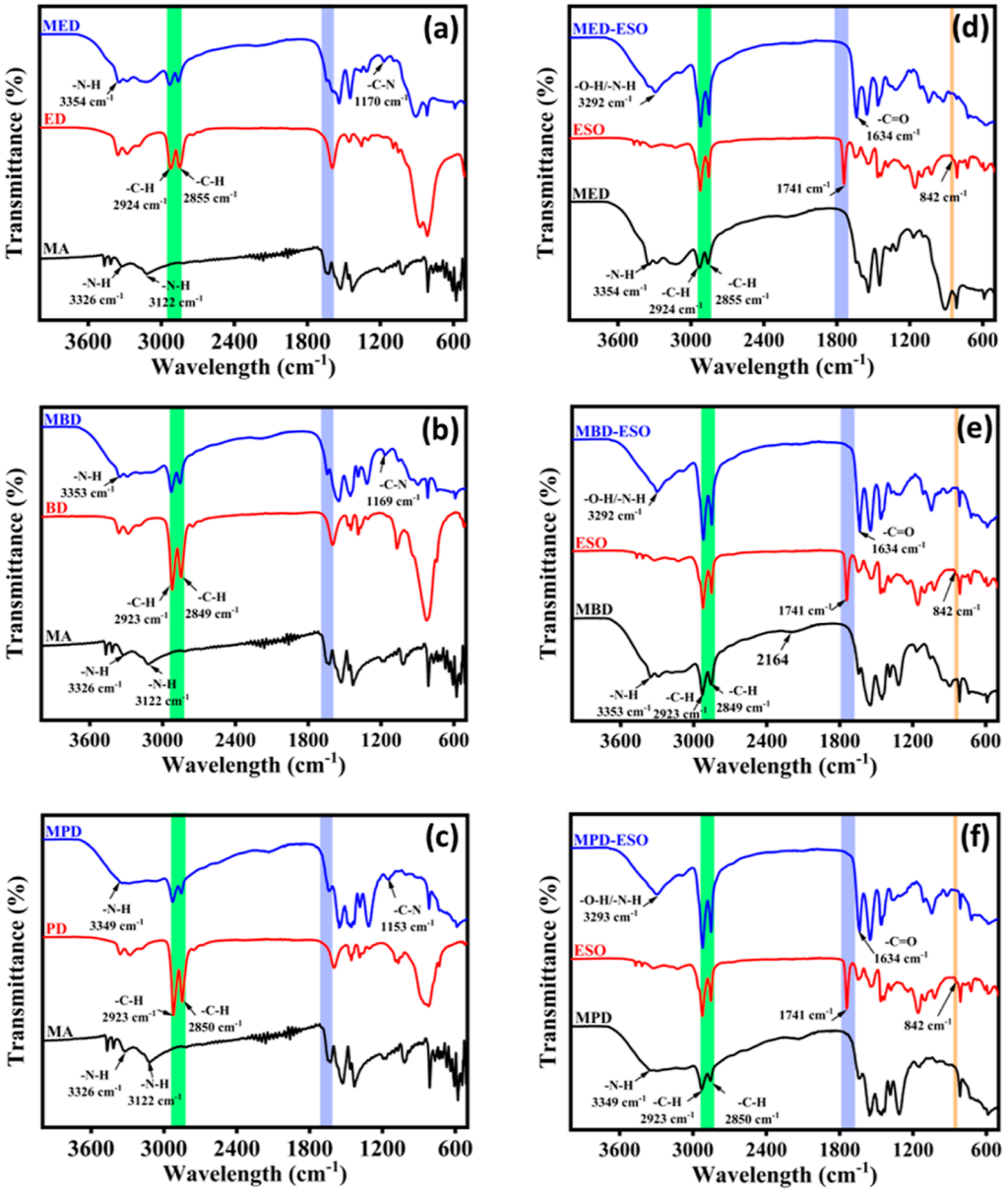

Figure 3. FT-IR spectra of (a) MED polymer, (b) MBD polymer, (c) MPD polymer, (d) MED-ESO resin, (e) MBD-ESO resin, and (f) MPD-ESO resin.

°C and maintained for 12 h. A similar procedure was adapted for the synthesis of MBD and MPD polymers. BDA and PDA were used for the synthesis of MBD and MPD polymers.

2.1.2. Synthesis of MED-ESO, MBD-ESO, and MPD-ESO Resins. Soybean oil was epoxidized using our previous method.[30] For the synthesis of MED-ESO resin, MED and ESO were mixed in 1:1 proportion, and the mixture was heated to 150 °C under stirring and maintained at this temperature for 2 h. A similar procedure was adapted for the synthesis of MBD-ESO and MPD-ESO resins but used MBD and MPD, respectively, and the products were also characterized by ^{1}H NMR (Figures S1−S3). During the reaction between MA-based polymers and ESO, two types of reactions may occur due to steric hindrance and the reactivity of triglycerides in ESO, as shown in the mechanism (Figure 2). In the first stage of amidation, a lone pair of terminals $-NH_2$ group tried to break the carbonyl part of triglyceride and make an amide bond, whereas in the second stage, a very sensitive epoxy group broke down and followed the ring opening reaction. In the MA-based polymer, chain length was increased (MED < MBD < MPD), and thus the steric hindrance was decreased, which led toward higher cross-linking.

2.1.3. Preparation of the Adhesive Specimen. To prepare the adhesive specimen, aluminum, copper, and stainless steel with a 25 mm × 25 mm (length × width) area were used, and adhesive was applied to the surface of each specimen.

2.2. Characterization. The structural analysis of the synthesized materials was performed using Fourier-transform infrared spectroscopy. FT-IR spectra were recorded using a PerkinElmer Spectrometer (Spectrum Two) in transmission mode (4000−500 cm^{-1}). The thermal behavior of the prepared samples was studied using thermogravimetric analysis (TGA) and differential scanning calorimetry (DSC). TGA was performed using TGA Q500 (TA Instruments, USA) under a nitrogen atmosphere at a 10 °C/min heating rate. DSC was performed using Q100 instruments (TA Instruments, USA).

https://doi.org/10.1021/acsomega.3c09650
ACS Omega 2024, 9, 10738−10747

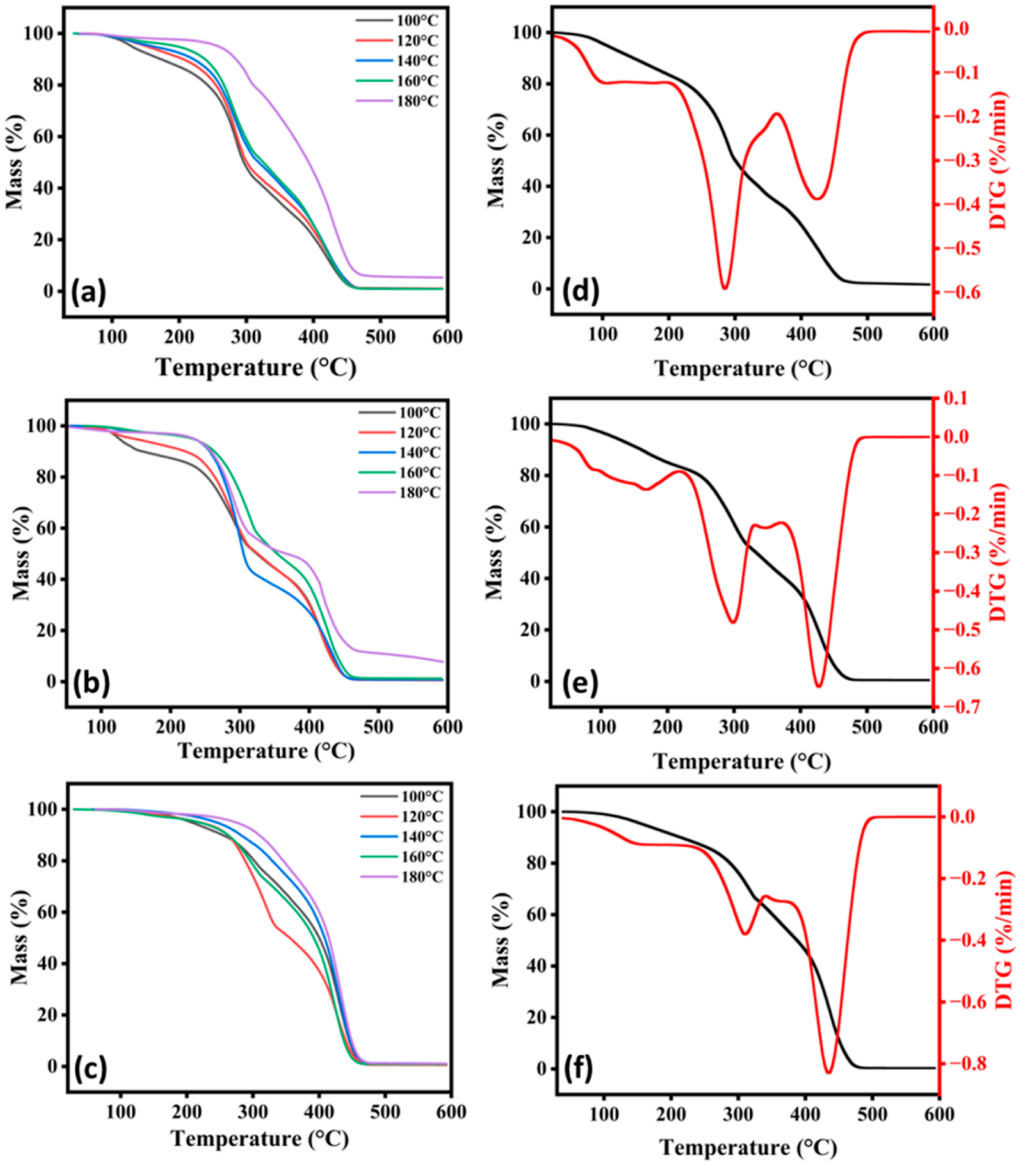

Figure 4. TGA spectra of (a) MED-ESO resin, (b) MBD-ESO resin, and (c) MPD-ESO resin, and derivative graphs of (d) MED-ESO resin, (e) MBD-ESO resin, and (f) MPD-ESO resin.

The samples were tested at a rate of 3 °C/min, 1 Hz frequency, and an amplitude of 10 μm. Lap shear and wet bonding were measured using an Instron 3367 instrument at room temperature and a crosshead speed of 500 mm/min.

3. RESULTS AND DISCUSSION

3.1. Fourier Transform Infrared Spectra. Figure 3 depicts the FT-IR spectra of the various materials. The stretching vibrations of N−H bonds show up as two weak peaks at 3122 and 3326 cm^{-1} for pure MA.[31] The symmetric vibration of $-CH_2-$ is attributed to the peaks at 2855 cm^{-1}, 2844 cm^{-1}, and 2850 cm^{-1} in EDA, BDA, and PDA, whereas the asymmetric vibration of $-CH_2-$ is attributed to the peaks at 2924 cm^{-1}, 2922 cm^{-1}, and 2923 cm^{-1}, respectively,[32] which became weaker in MED, MBD, and MPD polymers. In epoxidized soyabean oil, the peak at 842 cm^{-1} is assigned to the out-of-plane deformation, whereas the peak at 1743 cm^{-1} represents stretching of the triglyceride carbonyls of ESO,[33] almost vanished in the final product, and the additional peak is found at around 1637 cm^{-1}, attributed to the amide carbonyl (−NH−C═O) stretching,[33] indicates that ester bonds have been converted into amide connections as a result of processes involving aliphatic amino groups and triglyceride. More specifically, the C−N stretching peak and the NH_2 bending peak of MED, MBD, and MPD polymers are observed between 1100 and 1700 cm^{-1}. In addition, the N−H stretching vibration displays a peak at around 3350 cm^{-1} in all three samples. Peaking at 2210 cm^{-1}, the C−N group stretch in MED polymer indicates that the conversion from nitrile to pyridine structure is incomplete.[34] The peaks for symmetric CH_2 stretch and asymmetric CH_2 stretch are present at 2850 and 2920 cm^{-1} in all three resins.[35] The N−H stretching vibration accounts for the additional peak at 3300 cm^{-1} in MBD-ESO and MPD-ESO resin.[31]

3.2. Thermal Behavior of the Adhesives. The thermal decomposition behavior of all three polymers under nitrogen flow is shown in Figure 4. Moreover, the TGA thermogram and its derivatives of MED-ESO, MBD-ESO, and MPD-ESO resin, which are cured at 180 °C, are shown in Figure 4d−f.

https://doi.org/10.1021/acsomega.3c09650
ACS Omega 2024, 9, 10738−10747

The 5% mass loss ($T_{5\%}$) was found at 256, 233, and 276 °C, whereas 10% mass loss ($T_{10\%}$) was observed at 284, 258, and 308 °C in MED-ESO resin, MBD-ESO resin, and MPD-ESO resin, respectively. The degradations were found in three regions. In the 100−200 °C region, the minimum degradation was found due to the evaporation of small molecules like water and glycerol. While the second one is located between 200 and 400 °C, which could be attributed to the dissociation of larger molecules like fatty acid, the maximum mass loss (T_{max}) was also found in this region in MED-ESO resin. For MBD-ESO resin and MPD-ESO resin, the maximum mass loss (T_{max}) was found in the third region between 400 and 500 °C.

A differential scanning colorimetry study was performed (Figure 5) to estimate the T_g that defines the highest service temperature for the cured resins. From about 20−33 °C, MED-ESO resin goes through an endothermic reaction. Since rapid endothermicity was detected at 26.99 °C, this temperature is likely to represent the glass transition point for MED-ESO resin. For MBD-ESO resin, T_g was found at 19.11 °C in the temperature region from 13 to 27 °C. Moving forward to MPD-ESO resin, T_g was observed at 11.39 °C in the rapid exothermic curve from 7 to 19 °C. There was not any other thermal transition observed in the studied temperature range, suggesting the amorphous nature of all the samples.

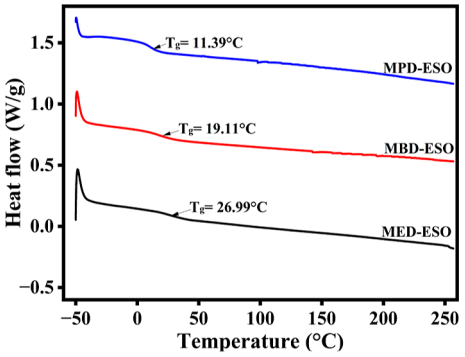

Figure 5. DSC spectra of MED-ESO, MBD-ESO, and MPD-ESO resin. (B) Chromophore-based ligand.

Out of all the polymeric materials, MED-ESO has a greater glass transition temperature, which decreases as the aliphatic chain of diamines increases. Polymers with a larger molecular weight often exhibit stronger intermolecular forces, resulting in an increased T_g value. However, MPD-ESO, due to its rubbery behavior caused by a longer aliphatic chain, has a reduced T_g value, perhaps due to enhanced material mobility. Therefore. It enhances the flexibility of the material. Therefore, there is an observed decrease in T_g values, with the trend being MED-ESO > MBD-ESO > MPD-ESO.

3.3. Adhesive Strengths of the Resins. *3.3.1. Dry Lap Shear Strength.* Figure 6 displays the dry lap shear strength of the three different resins. It is recommended that one give serious thought to replacing petroleum-based epoxy resins with EPO-based thermosetting resins in structural adhesives. Epoxy resins derived from petroleum can be used as structural solid adhesives, which is common knowledge. However, thermosets based on EPO that can be used as structural adhesives are not widely reported. We have done some testing to see how resin adheres at various temperatures. Stainless steel bonding strength guides our selection of curing time and temperature.

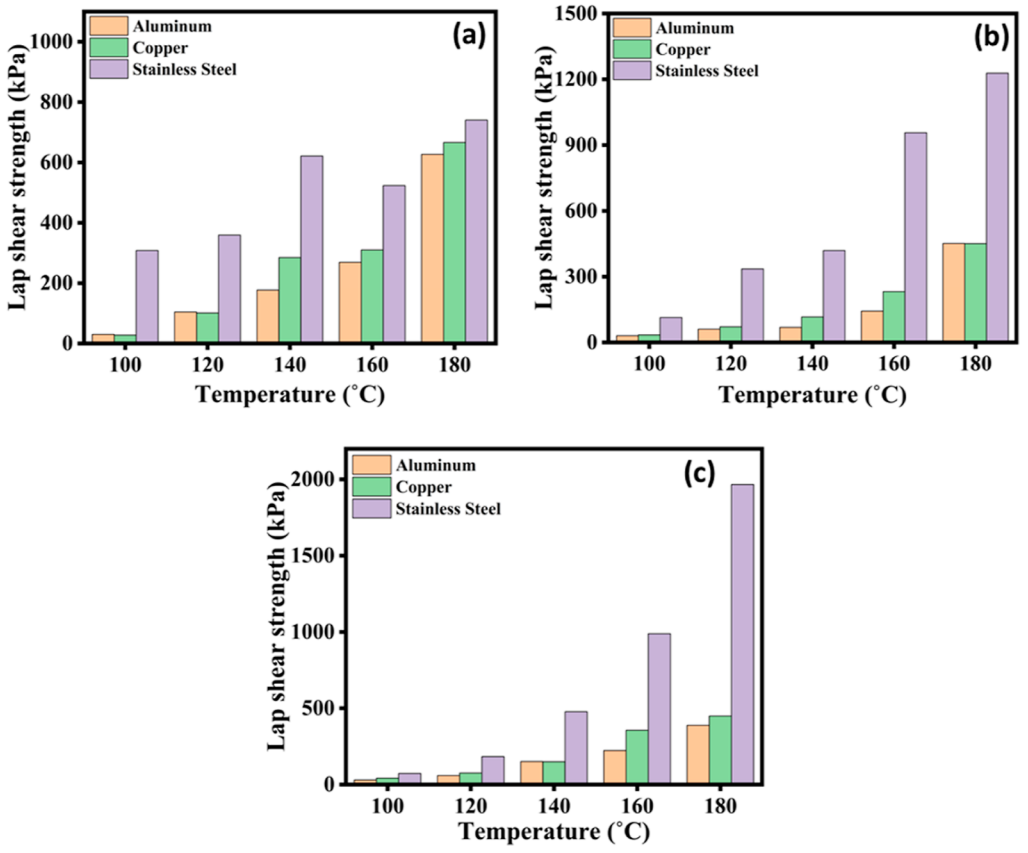

Figure 6. Lap shear of (a) MED-ESO, (b) MBD-ESO, and (c) MPD-ESO resins for three different metal sheets.

https://doi.org/10.1021/acsomega.3c09650
ACS Omega 2024, 9, 10738−10747

Table 1. Comparison of Mechanical Strength with Other Published Work

oil	starting material	substrate	tensile strength (kPa)	refs
canola	p-MDI	wood	5700	36
jatropha	TDI	wood	4900	37
castor	MDI, Nvoc-Cl, cadaverine	polyethylene	4600	38
acrylated ESO	3,4 dihydroxybenzoic acid	glass	2800	39
soyabean meal	HBAP, TGA, TA@G	wood	2590	40
acrylated linseed oil	PETMP	poplar wood	870	41
acrylated linseed oil	TMTMP	poplar wood	800	41
acrylated linseed oil	DiPETMP	wood	920	41
acrylated epoxidized soyabean oil	5-mercaptoisophthalic acid	stainless steel	1900	42
acrylated epoxidized soyabean oil	5-mercaptoisophthalic acid, microcrystalline cellulose	stainless steel	2400	42
epoxidized camelia oil	4-{[3-(thymin-1-yl)propanoyl]oxy}butyl acrylate, methoxy polyethylene glyco	ceramic	340	43
soya protein	acrylic acid	wood	1300	44
soya protein	acrylic acid, calcium sulfoaluminate	wood	1900	44
soyabean protein	acrylamide	wood	1000	45
soyabean protein	acrylamide, tannic acid	wood	1290	45
epoxidized soyabean oil	urea formaldehyde	wood	1880	46
plant oil	vinyl acetate	wood	1500	47
epoxide soyabean oil	MA, EDA	stainless steel	750	this work
epoxide soyabean oil	MA, BDA	stainless steel	1220	this work
epoxide soyabean oil	MA, PDA	stainless steel	1966	this work

We have tested times between 10 and 100 min and found that 60 min produced the best outcomes, and for 80 and 100 min, this material may undergo thermal degradation when exposed to high temperatures for an extended duration. This can result in changes to the molecular structure, reducing the material's mechanical properties. Hence, no adhesion was observed for 80 and 100 min. So, we have carried forward with 60 min of curing time for all the samples before performing our tensile tests. All the samples were glued with manual force using clamps. The bond strength of resin generally improved as the temperature was raised for all tested samples. MED-ESO resin steel, compared to other samples, has the best strength at all temperatures. Steel has a lap shear strength of about 300 kPa, which is more than 100% of copper and 100% of aluminum at 100 °C, although copper and aluminum both have a lap shear strength of less than 25 kPa. The lap shear strength increased by 750 kPa when the temperature was raised from 100 to 180 °C. Moreover, in MBD-ESO resin, at temperatures between 100 and 180 °C, the lap shear strength can reach 1220 kPa. Steel has the highest lap shear strength compared to aluminum and copper. At 180 °C, steel's lap shear strength was measured at 1220 kPa, while the greatest value measured for aluminum and copper was 450 kPa at the same temperature. The bonding strength of steel to the MPD-ESO polymer, at 100 °C, varies between 30 and 72 kPa for all metals. Steel had the highest lap shear strength of all samples tested (up to 1966 kPa) between 100 and 180 °C. All the samples became black and gritty when heated to 180 °C, most likely owing to oxidation. Interestingly, tensile strength was observed to be different on different metal coupons because there is a possibility that our synthesized material contains unreacted NH_2 terminal groups from diamines and OH groups resulting from the breakage of epoxy bonds of ESBO. The NH_2 group can chemically interact with metal oxides on the surface of a metal coupon, hence influencing the tensile strength. In addition, the NH_2 group can engage in surface activation, therefore improving the adhesive's wetting on the metal surface. Enhanced wetting leads to an increased contact area between the adhesive and the metal, perhaps resulting in greater adherence. Moreover, the existence of hydroxyl (OH) groups in the adhesive might result in hydrogen bonding interactions with the polar groups of the metal surface. Therefore, this can also enhance the bonding force. Regarding our findings, the adhesion strength of stainless steel has demonstrated the greatest adhesion strength compared with other metal samples. This might be attributed to the presence of chromium and iron oxide layers, which provide opportunities for hydrogen bonding with OH groups. Consequently, this interaction contributes to an increase in tensile strength. Essentially, stainless steel is more likely to have a higher concentration of oxidative groups compared to aluminum and copper, as it primarily consists of a blend of chromium and iron. This work is compared with other published work in the manner of mechanical strength, as shown in Table 1, and our result is better as compared to others as it is isocyanate and solvent-free.

3.3.2. Wet Lap Shear Strength. The best sample of dry lap shear strength was selected to perform wet lap shear strength on a stainless-steel metal coupon. Wet bonding strengths were monitored over the course of 3 h in cold water to assess the water resistance of the MED-ESO, MBD-ESO, and MPD-ESO resins. Wet bonding strengths are maximum after 1 h for all resins, with MPD showing the best strength at 1990 kPa (Figure 7). It is also confirmed from the DSC spectra that these polymeric materials are suitable for lower temperatures.

3.3.3. Gel Content. All the ESO resin which was cured at 180 °C was chosen (0.5 g) for the gel content test with three types of different solvents: tetrahydrofuran (THF), water, and toluene. All of the samples were kept in solvent for 24 h at room temperature. After 24 h sample was removed and dried at 50 °C for another 24 h for all the solvents, which is shown in Figure S4. After swelling in MED-ESO resin, weight loss was observed to 0.4 g in water solvent, which is a polar solvent. However, in THF, it showed the highest weight loss, from 0.5 to 0.14 g. In toluene, it is at 0.40, so no major loss was observed as compared to it in THF. While in MBD-ESO resin, loss of weight was observed at 0.43, 0.18, and 0.48 g,

https://doi.org/10.1021/acsomega.3c09650
ACS Omega 2024, 9, 10738−10747

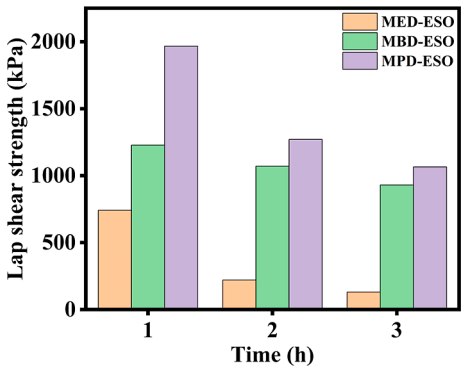

Figure 7. Wet bonding strengths of three different resins.

respectively, in water, THF, and toluene. Here, THF has shown the highest weight loss after gel content. The same trend was observed in MPD-ESO resin weight at 0.49, 0.06, and 0.36 g. In all of the samples, after curing at 50 °C, weight loss was negligible. So, it is concluded that there is no effect of weight loss on swollen material after drying at a certain temperature. From Figure 8, all the samples were more

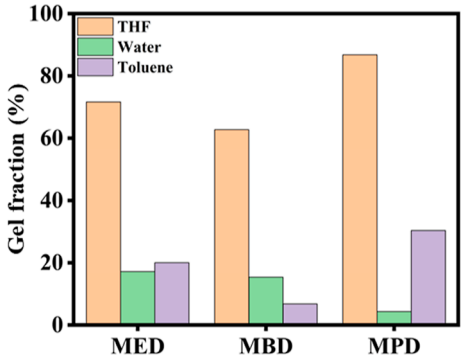

Figure 8. Gel fraction of three different resins in THF, water, and toluene.

dissolved in THF (>60%) as compared to other solvents. MPD-ESO resin shows the highest solubility in THF among all samples, which is 86%. It is interestingly observed that in water, as the number of aliphatic carbons in resin increased, the solubility decreased to 17, 15, and 4% for MED, MBD, and MPD resin, respectively, so it concludes that our polymeric materials are not polar as they were not dissolved in high amount as other solvents. However, in toluene, the trend was changed, and MPD resin shows the highest solubility at 30%, compared to 6 and 19% in MBD and MED resins, respectively. After gel content, the FT-IR spectra are also carried out, but no significant changes are found (Figure S5). All the adhesive materials have shown different gel percentages in different solvents because of differences in the chain length of diamines. It should be increased in THF from MED-ESO to MPD-ESO, but it was decreased in MBD-ESO, which may be due to either lower cross-linking or unreactivity of starting materials. The same trend was also observed for all the samples in the nonpolar solvent toluene. However, it is decreasing from MED-ESO to MPD-ESO in water as it is a polar aprotic solvent. Overall, the gel percentage in different solvents for adhesive materials is a result of a complex interaction between the polymer and the solvent. However, the chain length of diamines also plays a part in solubility, so different values of gel content are observed for all the polymeric materials in different solvents.

After the gel content test, major changes are observed in the thermal decomposition behavior of samples, which is confirmed by derivative thermograms (Figure 9). In MED-ESO resin, the maximum mass loss is changed from 200 to 400 °C for residual decomposition to 400−500 °C for the decomposition of larger molecules. It happens because smaller molecules of the polymer were dissolved in water during the gel content test. So, the bigger remaining part shows high thermal degradation. Moreover, the decomposition of larger molecules is found to decrease in both MBD-ESO resin and MPD-ESO resin in the same temperature range.

After gel content, a differential scanning colorimetry study was performed on the samples which were used in gel content for water solvent (Figure 10). The glass transition temperature of all the samples decreases upon the addition of a solvent. This is due to the penetration of solvent molecules into the polymer matrix, which disrupts the intermolecular forces responsible for maintaining the polymer's structure. This disturbance results in an enhancement in molecular mobility, enabling the polymer chains to experience more freedom of movement. Consequently, the glass transition temperature falls due to the polymer undergoing a transition to a less rigid state at a lower temperature. From 7 to 17 °C, MED-ESO resin goes through an endothermic reaction; this temperature range was decreased after gel content, and rapid endothermicity was observed at 12.54 °C; this temperature is likely to represent the glass transition point for MED-ESO resin after gel content. In short, it inclined toward 0 °C, so it has more flexibility. As such, in MBD-ESO resin, T_g is found at −0.70 °C in the temperature region from −7 to 4 °C of the endothermic process, so this polymer has the lowest T_g temperature among all, which shows the highest flexibility. Now, moving forward to the MPD-ESO resin, T_g is observed at 5.12 °C in the rapid exothermic curve from 0 to 8 °C. So, all the samples are more flexible at their Tg after gel content, and all are amorphous as before gel content.

4. CONCLUSIONS

The novel resin developed in this study is the result of a simple and environmentally friendly method of cross-linking ESO with highly branched and flexible polyamine via ring-opening and amidation polymerizations, which resulted in a material with novel features and broad potential uses. This material has shown not only good dry lap shear strength but also good wet lap shear strength, with a bonding strength of almost 2000 kPa for steel metal. After curing, MPD stayed as the strongest structural adhesive among the synthesized resins. This was on the same level as the performance of conventional petroleum-derived epoxy resins but far superior to the performance of other reported oil-based resins. When the strength of various samples of MED-ESO resin is compared, steel comes out on top regardless of the temperature. The variation in tensile strength among metal coupons is due to the existence of unreacted NH_2 and OH groups in our synthesized material. The NH_2 groups' interaction with metal oxides affects the tensile strength and enhances adhesive wetting. Hydroxyl groups contribute to the reinforcement of a substance by forming hydrogen bonds. Stainless steel, which contains chromium and iron oxide layers, has excellent adhesion strength due to its high concentration of oxidative groups. Compared to copper and aluminum, steel's lap shear strength

https://doi.org/10.1021/acsomega.3c09650
ACS Omega 2024, 9, 10738−10747

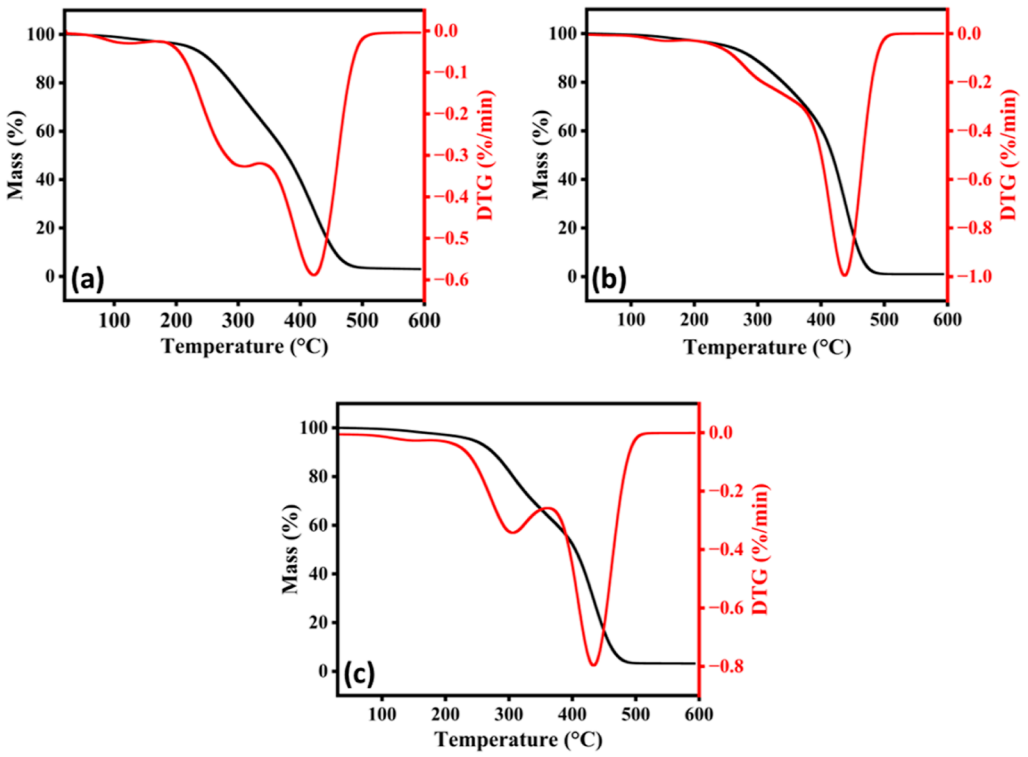

Figure 9. TGA of (a) MED-ESO, (b) MBD-ESO, and (c) MPD-ESO resins after gel fraction studies.

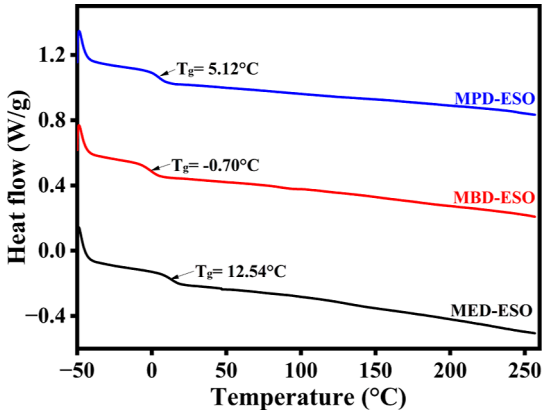

Figure 10. DSC spectra of the MED-ESO, MBD-ESO, and MPD-ESO resins after gel content studies.

of around 300 kPa is significantly higher at 100 °C, and it increases by another 750 kPa when heated to 180 °C. Comparatively, the shear strength of MBD-ESO resin at 180 °C is 1220 kPa, while that of MPD-ESO resin is 1996 kPa. From the gel content, it was confirmed that all the synthesized polymeric materials have shown less solubility in water, and MPD has shown the lowest solubility among all the samples. These materials have not shown any changes in FT-IR after performing the gel content. This is due to their higher strength and cross-linkage. In summary, at high temperatures (180 °C), all of the resins exhibit shear strengths comparable to steel.

■ ASSOCIATED CONTENT

Supporting Information

The Supporting Information is available free of charge at https://pubs.acs.org/doi/10.1021/acsomega.3c09650.

1H NMR spectrum of MED-ESO, MBD-ESO, and MPD-ESO, digital photo of MED-ESO, MBD-ESO, and MPD-ESO resins before and after gel content, and IR spectra of MED, MBD, and MPD resins after gel content (PDF)

■ AUTHOR INFORMATION

Corresponding Author

Ram K. Gupta − *Department of Chemistry, Pittsburg State University, Pittsburg, Kansas 66762, United States; National Institute for Materials Advancement, Pittsburg State University, Pittsburg, Kansas 66762, United States;* orcid.org/0000-0001-5355-3897; Email: ramguptamsu@gmail.com

Authors

Uday Panchal − *Department of Chemistry, Pittsburg State University, Pittsburg, Kansas 66762, United States; National Institute for Materials Advancement, Pittsburg State University, Pittsburg, Kansas 66762, United States*

Mayankkumar L. Chaudhary − *Department of Chemistry, Pittsburg State University, Pittsburg, Kansas 66762, United States; National Institute for Materials Advancement, Pittsburg State University, Pittsburg, Kansas 66762, United States*

Pratik Patel − *Department of Chemistry, Pittsburg State University, Pittsburg, Kansas 66762, United States; National Institute for Materials Advancement, Pittsburg State University, Pittsburg, Kansas 66762, United States*

Jainishkumar Patel − *Department of Chemistry, Pittsburg State University, Pittsburg, Kansas 66762, United States; National Institute for Materials Advancement, Pittsburg State University, Pittsburg, Kansas 66762, United States*

Complete contact information is available at:

https://doi.org/10.1021/acsomega.3c09650
ACS Omega 2024, 9, 10738−10747

https://pubs.acs.org/10.1021/acsomega.3c09650

Notes

The authors declare no competing financial interest.

■ ACKNOWLEDGMENTS

Authors acknowledge Pittsburgh State University for providing research and financial support.

■ REFERENCES

(1) Andrady, A. L.; Neal, M. A. Applications and societal benefits of plastics. *Philos. Trans. R. Soc. B Biol. Sci.* **2009**, *364*, 1977−1984.
(2) Hussain, F.; Hojjati, M.; Okamoto, M.; Gorga, R. E. Review article: Polymer-matrix Nanocomposites, Processing, Manufacturing, and Application: An Overview. *J. Compos. Mater.* **2006**, *40*, 1511−1575.
(3) Siracusa, V.; Rocculi, P.; Romani, S.; Rosa, M. D. Biodegradable polymers for food packaging: a review. *Trends Food Sci. Technol.* **2008**, *19*, 634−643.
(4) Meier, M. A. R.; Metzger, J. O.; Schubert, U. S. Plant oil renewable resources as green alternatives in polymer science. *Chem. Soc. Rev.* **2007**, *36*, 1788−1802.
(5) Sharma, V.; Kundu, P. P. Addition polymers from natural oils-A review. *Prog. Polym. Sci.* **2006**, *31*, 983−1008.
(6) Kim, H. N.; Guo, Z.; Zhu, W.; Yoon, J.; Tian, H. Recent progress on polymer-based fluorescent and colorimetric chemosensors. *Chem. Soc. Rev.* **2011**, *40*, 79−93.
(7) Guo, B.; Glavas, L.; Albertsson, A. C. Biodegradable and electrically conducting polymers for biomedical applications. *Prog. Polym. Sci.* **2013**, *38*, 1263−1286.
(8) Hu, J.; Zhu, Y.; Huang, H.; Lu, J. Recent advances in shape-memory polymers: Structure, mechanism, functionality, modeling and applications. *Prog. Polym. Sci.* **2012**, *37*, 1720−1763.
(9) Du, Y.; Shen, S. Z.; Cai, K.; Casey, P. S. Research progress on polymer-inorganic thermoelectric nanocomposite materials. *Prog. Polym. Sci.* **2012**, *37*, 820−841.
(10) Zhang, C.; Garrison, T. F.; Madbouly, S. A.; Kessler, M. R. Recent advances in vegetable oil-based polymers and their composites. *Prog. Polym. Sci.* **2017**, *71*, 91−143.
(11) Mu, Y.; Wan, X.; Han, Z.; Peng, Y.; Zhong, S. Rigid polyurethane foams based on activated soybean meal. *J. Appl. Polym. Sci.* **2012**, *124*, 4331−4338.
(12) Husic, S.; Javni, I.; Petrović, Z. S. Thermal and mechanical properties of glass reinforced soy-based pol yurethane composites. *Compos. Sci. Technol.* **2005**, *65*, 19−25.
(13) Seniha Güner, F.; Yağci, Y.; Tuncer Erciyes, A. Polymers from triglyceride oils. *Prog. Polym. Sci.* **2006**, *31*, 633−670.
(14) Miao, S.; Wang, P.; Su, Z.; Zhang, S. Vegetable-oil-based polymers as future polymeric biomaterials. *Acta Biomater.* **2014**, *10*, 1692−1704.
(15) Hu, L.; Khaniya, A.; Wang, J.; Chen, G.; Kaden, W. E.; Feng, X. Ambient Electrochemical Ammonia Synthesis with High Selectivity on Fe/Fe Oxide Catalyst. *ACS Catal.* **2018**, *8*, 9312−9319.
(16) Lei, Y. F.; Wang, X. L.; Liu, B. W.; Ding, X. M.; Chen, L.; Wang, Y. Z. Fully Bio-Based Pressure-Sensitive Adhesives with High Adhesivity Derived from Epoxidized Soybean Oil and Rosin Acid. *ACS Sustain. Chem. Eng.* **2020**, *8*, 13261−13270.
(17) Wu, J.; Yu, X.; Zhang, H.; Guo, J.; Hu, J.; Li, M.-H. Fully Biobased Vitrimers from Glycyrrhizic Acid and Soybean Oil for Self-Healing, Shape Memory, Weldable, and Recyclable Materials. *ACS Sustain. Chem. Eng.* **2020**, *8*, 6479−6487.
(18) Wang, Z.; Zhang, X.; Wang, R.; Kang, H.; Qiao, B.; Ma, J.; Zhang, L.; Wang, H. Synthesis and Characterization of Novel Soybean-Oil-Based Elastomers with Favorable Processability and Tunable Properties. *Macromolecules* **2012**, *45*, 9010−9019.
(19) Intarabumrung, W.; Kuntharin, S.; Harnchana, V.; Prada, T.; Kasemsiri, P.; Hunt, A. J.; Supanchaiyamat, N. Facile Synthesis of Biobased Polyamide Derived from Epoxidized Soybean Oil as a High-Efficiency Triboelectric Nanogenerator. *ACS Sustain. Chem. Eng.* **2022**, *10*, 13680−13691.
(20) Yang, H.; Du, G.; Li, Z.; Ran, X.; Zhou, X.; Li, T.; Gao, W.; Li, J.; Lei, H.; Yang, L. Superstrong Adhesive of Isocyanate-Free Polyurea with a Branched Structure. *ACS Appl. Polym. Mater.* **2021**, *3*, 1638−1651.
(21) Omonov, T. S.; Patel, V. R.; Curtis, J. M. Biobased Thermosets from Epoxidized Linseed Oil and its Methyl Esters. *ACS Appl. Polym. Mater.* **2022**, *4*, 6531−6542.
(22) Fang, X.; Tian, N.; Hu, W.; Qing, Y.; Wang, H.; Gao, X.; Qin, Y.; Sun, J. Dynamically Cross-Linking Soybean Oil and Low-Molecular-Weight Polylactic Acid toward Mechanically Robust, Degradable, and Recyclable Supramolecular Plastics. *Adv. Funct. Mater.* **2022**, *32*, 2208623.
(23) Qi, M.; Xu, Y. J.; Rao, W. H.; Luo, X.; Chen, L.; Wang, Y. Z. Epoxidized soybean oil cured with tannic acid for fully bio-based epoxy resin. *RSC Adv.* **2018**, *8*, 26948−26958.
(24) Yang, X.; Wang, S.; Liu, X.; Huang, Z.; Huang, X.; Xu, X.; Liu, H.; Wang, D.; Shang, S. Preparation of non-isocyanate polyurethanes from epoxy soybean oil: Dual dynamic networks to realize self-healing and reprocessing under mild conditions. *Green Chem.* **2021**, *23*, 6349−6355.
(25) Li, C.; Ju, B.; Zhang, S. Fully bio-based hydroxy ester vitrimer synthesized by crosslinking epoxidized soybean oil with doubly esterified starch. *Carbohydr. Polym.* **2023**, *302*, 120442.
(26) Liu, X.; Yang, X.; Wang, S.; Wang, S.; Wang, Z.; Liu, S.; Xu, X.; Liu, H.; Song, Z. Fully Bio-Based Polyhydroxyurethanes with a Dynamic Network from a Terpene Derivative and Cyclic Carbonate Functional Soybean Oil. *ACS Sustain. Chem. Eng.* **2021**, *9*, 4175−4184.
(27) Wang, T.; Deng, H.; Li, N.; Xie, F.; Shi, H.; Wu, M.; Zhang, C. Mechanically strong non-isocyanate polyurethane thermosets from cyclic carbonate linseed oil. *Green Chem.* **2022**, *24*, 8355−8366.
(28) Baghban, S. A.; Ebrahimi, M.; Khorasani, M. A facile method to synthesis of a highly acrylated epoxidized soybean oil with low viscosity: Combined experimental and computational approach. *Polym. Test.* **2022**, *115*, 107727.
(29) Yuan, J.; Du, G.; Yang, H.; Liu, S.; Wu, Y.; Ni, K.; Ran, X.; Gao, W.; Yang, L.; Li, J. Functionalization of cellulose with amine group and cross-linked with branched epoxy to construct high-performance wood adhesive. *J. Biol. Macromol.* **2022**, *222*, 2719−2728.
(30) Suthar, V.; Asare, M. A.; Sahu, P.; Gupta, R. K. Sunflower oil-based polyurethane/graphene composite: Synthesis and properties. *J. Thermoplast. Compos. Mater.* **2023**, 08927057231202408.
(31) Yuan, X.; Luo, K.; Zhang, K.; He, J.; Zhao, Y.; Yu, D. Combinatorial vibration-mode assignment for the FTIR spectrum of crystalline melamine: A strategic approach toward theoretical IR vibrational calculations of triazine-based compounds. *J. Phys. Chem. A* **2016**, *120*, 7427−7433.
(32) Singh, K.; Ohlan, A.; Saini, P.; Dhawan, S. K. Poly (3,4-ethylenedioxythiophene) γ-Fe2O3 polymer composite - super paramagnetic behavior and variable range hopping 1D conduction mechanism - synthesis and characterization. *Polym. Adv. Technol.* **2008**, *19*, 229−236.
(33) Qian, Z.; Liu, S.; Du, G.; Wang, S.; Shen, Y.; Zhou, X.; Jiang, S.; Niu, H.; Duan, Z.; Li, T. Versatile Epoxidized Soybean Oil-Based Resin with Excellent Adhesion and Film-Forming Property. *ACS Sustain. Chem. Eng.* **2023**, *11*, 5315−5324.
(34) Zheng, W.; Hu, J.; Han, Z.; Wang, Z.; Zheng, Z.; Langer, J.; Economy, J. Synthesis of porous carbon fibers with strong anion exchange functional groups. *Chem. Commun.* **2015**, *51*, 9853−9856.
(35) Yang, W.; Wang, C.; Arrighi, V. An organic silver complex conductive ink using both decomposition and self-reduction mechanisms in film formation. *J. Mater. Sci. Mater. Electron.* **2018**, *29*, 2771−2783.
(36) Kong, X.; Liu, G.; Curtis, J. M. Characterization of canola oil based polyurethane wood adhesives. *Int. J. Adhes. Adhes.* **2011**, *31*, 559−564.

(37) Aung, M. M.; Yaakob, Z.; Kamarudin, S.; Abdullah, L. C. Synthesis and characterization of Jatropha (Jatropha curcas L.) oil-based polyurethane wood adhesive. *Ind. Crops Prod.* **2014**, *60*, 177−185.
(38) Borrero-López, A. M.; Guzmán, D. B.; González-Delgado, J. A.; Arteaga, J. F.; Valencia, C.; Pischel, U.; Franco, J. M. Toward UV-Triggered Curing of Solvent-Free Polyurethane Adhesives Based on Castor Oil. *ACS Sustain. Chem. Eng.* **2021**, *9*, 11032−11040.
(39) Xiong, G.; Xiong, W.; Dai, S.; Lin, M.; Xia, G.; Wan, X.; Mu, Y. Fast-Curing Mussel-Inspired Adhesive Derived from Vegetable Oil. *ACS Appl. Bio Mater.* **2021**, *4*, 1360−1368.
(40) Zhang, F.; Li, H.; Wang, T.; Li, X.; Li, K.; Aladejana, J. T.; Tian, D.; Li, J.; Li, J. Advanced Biomimetic Soybean Meal-Based Adhesive with High Strength and Toughness. *ACS Sustain. Chem. Eng.* **2022**, *10*, 17355−17368.
(41) Addis, C. C.; Koh, R. S.; Gordon, M. B. Preparation and characterization of a bio-based polymeric wood adhesive derived from linseed oil. *Int. J. Adhes. Adhes.* **2020**, *102*, 102655.
(42) Del Prado, A.; Hohl, D. K.; Balog, S.; De Espinosa, L. M.; Weder, C. Plant Oil-Based Supramolecular Polymer Networks and Composites for Debonding-on-Demand Adhesives. *ACS Appl. Polym. Mater.* **2019**, *1*, 1399−1409.
(43) Yan, Y.; Wu, J.; Wang, Y.; Fang, X.; Wang, Z.; Yang, G.; Hua, Z. Strong and UV-Responsive Plant Oil-Based Ethanol Aqueous Adhesives Fabricated Via Surfactant-free RAFT-Mediated Emulsion Polymerization. *ACS Sustain. Chem. Eng.* **2021**, *9*, 13695−13702.
(44) Pang, H.; Ma, C.; Shen, Y.; Sun, Y.; Li, J.; Zhang, S.; Cai, L.; Huang, Z. Novel Bionic Soy Protein-Based Adhesive with Excellent Prepressing Adhesion, Flame Retardancy, and Mildew Resistance. *ACS Appl. Mater. Interfaces* **2021**, *13*, 38732−38744.
(45) Pang, H.; Yan, Q.; Ma, C.; Zhang, S.; Gao, Z. Polyphenol-Metal Ion Redox-Induced Gelation System for Constructing Plant Protein Adhesives with Excellent Fluidity and Cold-Pressing Adhesion. *ACS Appl. Mater. Interfaces* **2021**, *13*, 59527−59537.
(46) Duan, Z.; Hu, M.; Jiang, S.; Du, G.; Zhou, X.; Li, T. Cocuring of Epoxidized Soybean Oil-Based Wood Adhesives and the Enhanced Bonding Performance by Plasma Treatment of Wood Surfaces. *ACS Sustain. Chem. Eng.* **2022**, *10*, 3363−3372.
(47) Liu, W.; Wu, M.; Ma, C.; Liu, C.; Zhang, X.; Wang, Z.; Wang, Z. Efficient Miniemulsion Polymerization of Plant Oil-Based Acrylate Monomer toward Waterborne Epoxy Resins. *ACS Sustain. Chem. Eng.* **2022**, *10*, 13301−13309.

https://doi.org/10.1021/acsomega.3c09650
ACS Omega 2024, 9, 10738−10747